International Research Journal of Pure & Applied Chemistry

22(8): 1-13, 2021; Article no.IRJPAC.74673
ISSN: 2231-3443, NLM ID: 101647669

Inhibition Effect of Atenolol on Copper Corrosion in 1M HNO_3: Experimental Study and DFT

Ehouman Ahissan Donatien[1*], Bamba Kafoumba[1], Kogbi Guy Roland[1], Bamba Amara[2], Kouakou Adjoumani Rodrigue[1] and Fatogoma Diarrassouba[1]

[1]Laboratoire de Thermodynamique et Physico-Chimie du Milieu, UFR SFA, Université NANGUI ABROGOUA, 02 BP 801 Abidjan 02, Côte-d'Ivoire.
[2]Laboratoire de Constitution et Réaction de la Matière, UFR SSMT, Université Félix Houphouët-Boigny, Abidjan Cocody, 22 BP 582 Abidjan 22, Côte-d'Ivoire.

Authors' contributions

This work was carried out in collaboration among all authors. All authors read and approved the final manuscript.

Article Information

DOI: 10.9734/IRJPAC/2021/v22i830423
Editor(s):
(1) Dr. Farzaneh Mohamadpour, University of Sistan and Baluchestan, Iran.
Reviewers:
(1) Archana Rao P, BVRIT Hyderabad College of Engineering for Women, India.
(2) Ziouche Aicha, University of Boumerdes, Algeria.
(3) K. Gurushankar, Kalasalingam Academy of Research and Education, India.
Complete Peer review History: https://www.sdiarticle4.com/review-history/74673

Original Research Article

Received 27 July 2021
Accepted 03 October 2021
Published 09 October 2021

ABSTRACT

Atenolol was examined as a copper corrosion inhibitor in 1M nitric acid solution using the mass loss technique and quantum chemical studies, based on density functional theory (DFT) at the B3LYP level with the base 6-311G (d,p). The inhibitory efficiency of the molecule increases with increasing concentration and temperature. The adsorption of the molecule on the copper surface follows the modified Langmuir model. The thermodynamic quantities of adsorption and activation were determined and discussed. The calculated quantum chemical parameters related to the inhibition efficiency are the energy of the highest occupied molecular orbital E(HOMO), the energy of the lowest unoccupied molecular orbital E(LUMO), the HOMO-LUMO energy gap, the hardness (η), softness (S), dipole moment (μ), electron affinity (A), ionization energy (I), absolute electronegativity (χ),absolute electronegativity (χ), fraction (ΔN) of electrons transferred from Atenolol to copper and electrophilicity index(ω). The local reactivity was analyzed through the condensed Fukui function and condensed softness indices to determine the nucleophilic and electrophilic attack sites. There is good agreement between the experimental and theoretical results.

**Corresponding author: E-mail: ehoumandona@gmail.com, dodolamour2000@yahoo.fr;*

Keywords: Atenolol; corrosion inhibition; copper; density functional theory (DFT); mass loss technique.

1. INTRODUCTION

Copper and its alloys [1,2] are widely used in various fields (shipbuilding, communications, piping, etc.) because of their excellent electrical and thermal conductivity. However, in contact with aggressive media, particularly acidic media, copper and its alloys dissolve (corrosion) [3,4], which has led many researchers to take an interest in inhibiting the corrosion of this metal and its alloys. One of the most widely used methods of protecting metals against corrosion is the use of organic corrosion inhibitors [5,6] which contain heteroatoms such as nitrogen, sulphur and oxygen; these compounds are usually heterocyclic [7,8] with polar functional groups and conjugated double bonds. The inhibitory action of these organic compounds is attributed to their interactions with the copper surface via their adsorption. The polar functional groups [9] are considered to be the reaction centers that stabilize the adsorption process. In general, the adsorption of an inhibitor on a metal surface [10] depends on the nature of the surface, the mode of adsorption, the molecular structure and the type of electrolyte solution. The general objective is to study the behavior of the drug atenolol and its efficiency towards the corrosion of copper in nitric acid medium. Previous studies on some antibiotics such as cefatrexyl and cefazolin have shown good inhibitory efficacy of iron in chlorine [11]. Thus, chemical drugs that are considered to be non-toxic are promising in the search for effective and inexpensive inhibitors against metal corrosion in acidic media.

2. MATERIALS AND METHODS

2.1 Copper Specimens

The copper samples were in the form of a rod 10 mm long and 2 mm in diameter. It is a commercial copper of 95.95% purity.

2.2 The Molecule Studied

Atenolol is a molecule of the beta-blocker class, used to treat high blood pressure, angina pectoris or myocardial infarction. Image 1 shows the molecular structure of Atenolol.

This work, which is a contribution to the study of metal corrosion inhibition in acidic media, aims to study the behaviour of atenolol towards copper corrosion in 1M nitric acid.
C_{14} H_{22} N_2 O_3.

Atenolol is a white or approximately white powder, fairly soluble in water and ethanol, with a molecular weight M=266,34 g.mol^{-1}.

2.3 Solution

An analytical grade 65% nitric acid solution from Merck was used to prepare the aqueous corrosive solution. The solution was prepared by diluting the commercial nitric acid solution with ultrapure water. The blank was a 1 M HNO_3 solution. The Atenolol solutions prepared were of concentrations 0,093 mM; 0,187 mM; 0,234 mM and 0,375 mM.

2.4 Mass Loss Method

Mass loss measurements were performed by total immersion of the pre-weighed copper sample in 100 mL capacity beakers containing 50 mL of the test solution maintained at a temperature of (298K to 323K). The samples were recovered one hour later and rinsed thoroughly with distilled water, cleaned, dried in acetone and reweighed using a balance with a sensitivity of ±0.1 mg. All tests were performed in triplicate to ensure reliability of the results. Weight loss was considered as the difference between the initial weight and the weight after 1 h of immersion. The average values of the mass loss data were used to calculate parameters such as corrosion rate, inhibition efficiency and surface coverage using the following relationships:

$$W = \frac{\Delta m}{St} \quad (1)$$

$$EI(\%) = \frac{W_0 - W}{W_0} \times 100 \quad (2)$$

$$\theta = \frac{W_0 - W}{W_0} \quad (3)$$

Where W_0 and W are the corrosion rate in the absence and presence of the inhibitor respectively Δm is the mass loss, S is the total surface area of the copper sample and t is the immersion time.

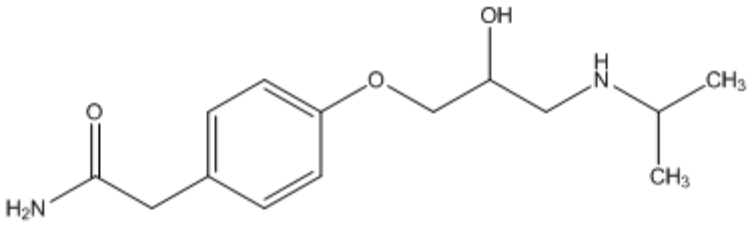

Image 1. Molecular structure of Atenolol

2.5 Quantum Calculations

Density functional theory (DFT) calculations were carried out involving various steps including a graphical representation of the geometry of the molecule using the Gaussview visualization interface, and the application of a theoretical method (DFT) implemented in the commercial software Gaussian. For our study, the geometrical optimization of our molecule was performed using the Density Functional Theory (DFT) method with the B3LYP functional [12] and the 6-311G (d,p) basis. The software GaussView 5.0 [13] was used to represent the 3D structure and visualize the molecule under study. The calculations were performed with the Gaussian 09 W software [14]. The relevant parameters were calculated to describe the molecule-metal interactions.

The basic relationship of the density functional theory of chemical reactivity is precisely, the one established by Parr et al [15] which links the chemical electron potential $\boldsymbol{\mu_P}$ to the first derivative of the energy with respect to the number of electrons $\boldsymbol{N}$, and thus with the negative of the electronegativity $\boldsymbol{\chi}$:

$$\boldsymbol{\mu_P} = \left(\frac{\partial E}{\partial N}\right)_{v(r)} = -\boldsymbol{\chi} \quad (4)$$

The hardness $\boldsymbol{\eta}$ which measures both the stability and reactivity of a molecule [16] has been defined as the second derivative of the total energy $\boldsymbol{E}$ with respect to $\boldsymbol{N}$ at constant external potential $\boldsymbol{v(r)}$:

$$\eta = \left(\frac{\partial^2 E}{\partial N^2}\right)_{v(r)} = \left(\frac{\partial \mu_P}{\partial N}\right)_{v(r)} \quad (5)$$

In these equations, is the chemical potential, $\boldsymbol{E}$ is the total energy, N is the number of electrons and $\boldsymbol{v(r)}$is the external potential.

According to Koopmans theorem [17], the ionization energy $\boldsymbol{I}$ can be approximated as the negative of the energy of the highest occupied molecular orbital (HOMO):

$$I = -E_{HOMO} \quad (6)$$

The negative of the lowest unoccupied molecular orbital energy (LUMO) is similarly related to the electronic affinity $\boldsymbol{A}$ as follows:

$$A = -E_{LUMO} \quad (7)$$

The electronegativity $\boldsymbol{\chi}$ and the hardness $\boldsymbol{\eta}$ can then be written as follows

$$\chi = \frac{I + A}{2} \quad (8)$$

$$\eta = \frac{I - A}{2} \quad (9)$$

The fraction of electrons transferred from the molecule to the metal [18] is expressed as follows:

$$\Delta N = \frac{\chi_{Cu} - \chi_{inh}}{2(\eta_{Cu} + \eta_{inh})} \quad (10)$$

The opposite of hardness is softness [19]

$$S = \left(\frac{\partial N}{\partial \mu_P}\right)_{v(r)} \quad (11)$$

The overall electrophilicity index ω introduced by Parr [20], which is a measure of the energy lowering due to maximum electron flow between the donor and acceptor, is given by:

$$\omega = \frac{\mu_P^2}{2\eta} \quad (12)$$

The local reactivity of the molecule under study can be analyzed by means of the fused Fukui indices. Condensed functions indicate the atoms in a molecule that tend to donate (nucleophilic character) or accept (electrophilic character) an electron or electron pair. The nucleophilic and

electrophilic functions can be calculated using the finite difference approximation as follows:

$$f_k^+ = [q_k(N+1) - q_k(N)] \quad (13)$$

$$f_k^- = [q_k(N) - q_k(N-1)] \quad (14)$$

In equations (13) and (14), q_k is the gross charge of atom k in the molecule and N is the number of electrons.

3. RESULTS AND DISCUSSION

3.1 Mass Loss Experiment

Mass loss data was determined at the end of a 1-hour time interval in the absence and presence of different concentrations of Atenolol and was used to calculate corrosion rates, inhibition efficiency and surface coverage, according to equations (1-3). Figs. 1 and 2 show the evolution of corrosion rate and inhibition efficiency as a function of temperature and Atenolol concentration, respectively.

Fig. 2 shows that the inhibitory efficiency of Atenolol increases with both temperature and inhibitor concentration. This could be explained by a higher copper surface coverage when the inhibitor concentration increases and especially by the formation of a Cu-Atenolol complex film (the vacant d-orbitals of the Cu^{2+} ions receive electrons from the Atenolol molecules. This leads to an increase in inhibitory efficiency as the temperature increases.

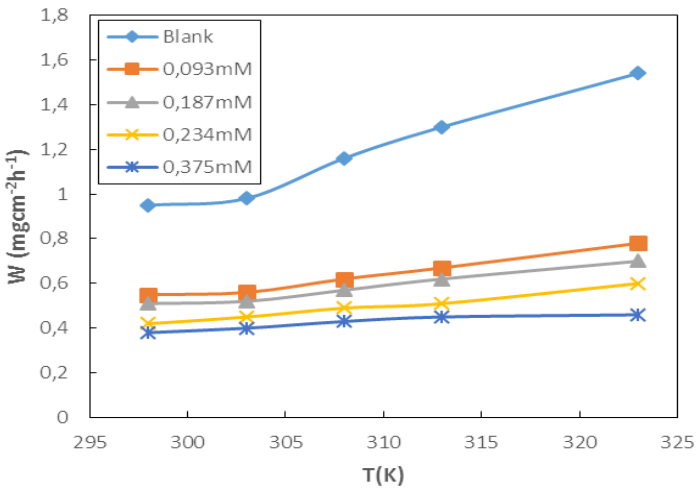

Fig. 1. Corrosion rate versus temperature curve for different concentrations of Atenolol

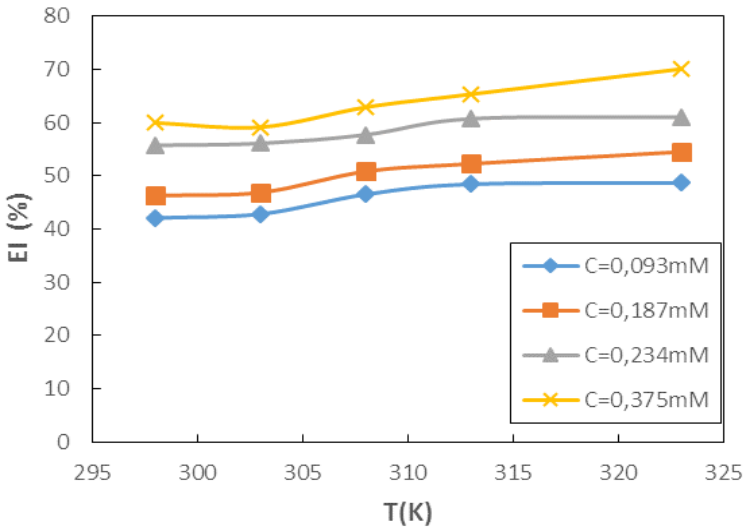

Fig. 2. Inhibition efficiency as a function of temperature for different concentrations of Atenolol

3.2 Adsorption Isotherm

The model that best fits the adsorption process was chosen using the values of the correlation coefficient R^2 of the graphs: the highest value of the correlation coefficient corresponds to the best model. The isotherm models in their respective modes are described by the following equation:

$$f(\theta, x)\exp(-2a\theta) = K_{ads}C_{inh} \quad (15)$$

Where $f(\theta, x)$ represents the configuration factor and depends on the physical model and the assumptions underlying the derivation of the model, θ is the metal surface coverage rate, , C_{inh} is the inhibitor concentration, a is a molecular interaction parameter, x is the number of water molecules replaced by an organic molecule, K_{ads} is the equilibrium constant of the adsorption process. The equations of the attempted models are listed in Table 1.

Table 1. Equations of the studied isotherms

Isotherme	Equations
Langmuir	$\frac{C_{inh}}{\theta} = \frac{1}{K_{ads}} + C_{inh}$
Temkin	$\theta = \frac{2{,}303}{-2a}[logK_{ads} + logC_{inh}]$
El-Awady	$log\left(\frac{\theta}{1-\theta}\right) = logK + y\, logC_{inh}$

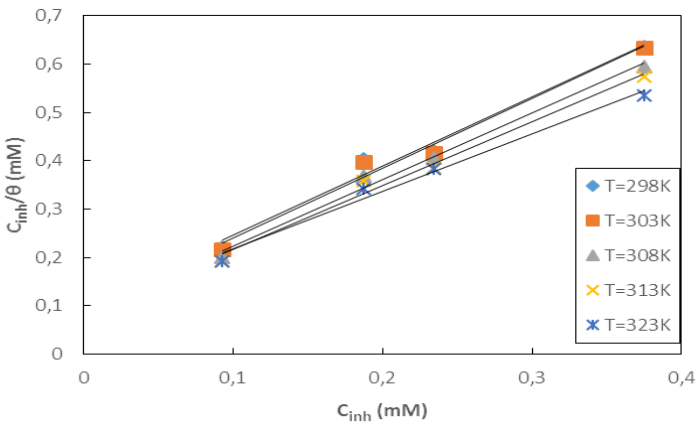

Fig. 3 A. Langmuir isotherms for the adsorption of Atenolol on copper in 1M HNO_3 medium at different temperatures

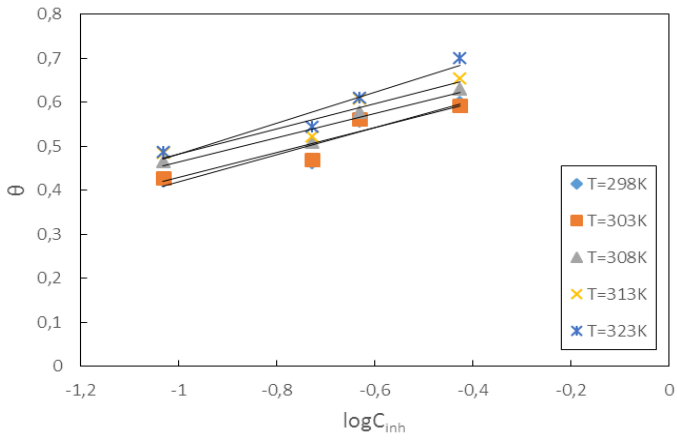

Fig. 3B. Temkin isotherms for the adsorption of Atenolol on copper in 1M HNO_3 medium at different temperatures

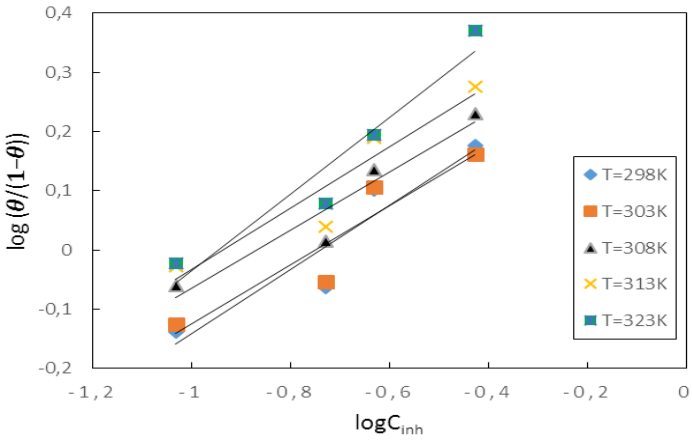

Fig. 3C. El-Awady isotherms for the adsorption of Atenolol on copper in 1M HNO_3 medium at different temperatures

Fig. 3. (A, B and C) shows the graphs of the isotherms studied

The Langmuir adsorption isotherm is by far the best isotherm (R^2 = 0.999, is almost equal to unity) but there is a divergence in the slope from unity [21] due to interactions between species adsorbed on the copper surface as well as changes in Gibbs energy values with increasing surface coverage. The results suggest a slight deviation from the ideal conditions (all adsorption sites are equivalent) assumed in the Langmuir model. Therefore, a modified Langmuir equation, suggested elsewhere [22] and presented in the equation below, which accounts for this deviation, can be used:

$$\frac{C_{inh}}{\theta} = \frac{n}{K} + nC_{inh} \quad (16)$$

$n\theta$ is the effective recovery rate.

The thermodynamic parameters can be determined using the relationship between the equilibrium constant K_ads and the change in free enthalpy of adsorption ΔG^0_{ads}

$$\Delta G^0_{ads} = -RTln(55{,}5K_{ads}) \quad (17)$$

Where R is the perfect gas constant, T is the absolute temperature and 55.5 is the concentration of water in $mol.L^{-1}$.

The values of ΔG^0_{ads} obtained are given in Table 2.

The values of ΔG^0_{ads} are negative for all temperatures explored; this means that the adsorption of Atenolol on copper is spontaneous. According to the literature [23], a value of ΔG^0_{ads} lower than -40 $kJ.mol^{-1}$ would indicate a chemical adsorption process (chemisorption) whereas a value higher than -20 $kJ.mol^{-1}$ would indicate a physical adsorption process (physisorption).For values between-40 $kJ.mol^{-1}$ and -20 $kJ.mol^{-1}$, both types of adsorption would exist. With regard to the values contained in the table, we can deduce that the adsorption of Atenolol on copper takes place according to the two adsorption modes (physisorption and chemisorption).

The variations in enthalpies ΔH^0_{ads} and entropy ΔS^0_{ads} of adsorption are deduced using the following equation:

$$\Delta G^0_{ads} = \Delta H^0_{ads} - T\Delta S^0_{ads} \quad (18)$$

Where ΔH^0_{ads} and ΔS^0_{ads} are respectively the y-intercept and the opposite of the slope of the straight line obtained from the curve of ΔG^0_{ads} versus temperature (Fig. 4).

Table 2. Values of thermodynamic quantities related to the adsorption of Atenolol on copper

T(K)	K_{ads} (× 10^3 M^{-1})	ΔG^0_{ads} ($kJ.mol^{-1}$)	ΔH^0_{ads} ($kJ.mol^{-1}$)	ΔS^0_{ads} ($J.mol^{-1}_{))})^1.K^{-1}$)
298	09.04	-32.72	7,24	134.3
303	10.25	-33,40		
308	11.35	-34,25		
313	11.50	-34,89		
323	12,22	-36,05		

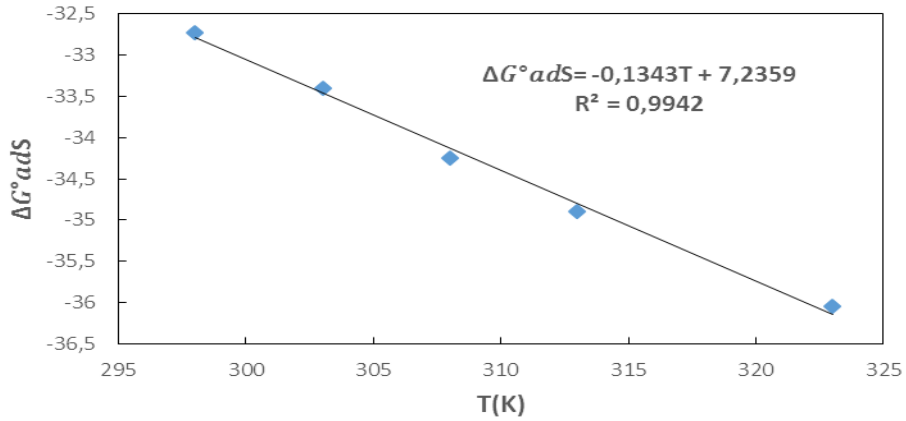

Fig. 4. Free enthalpy changes versus temperature

The adsorption enthalpy variation ΔH^0_{ads} has a positive value, reflecting the endothermic character of the adsorption process. The adsorption entropy variation ΔS^0_{ads} is positive, which indicates an increase in disorder during the adsorption of Atenolol on copper. This increase in disorder would be due to the desorption of water molecules.

3.3 Effect of Temperature

The thermodynamic activation quantities (activation energy E_a, activation enthalpy change ΔH^*_a and activation entropy change ΔS^*_a) for the corrosion process were determined from the Arrhenius and transition state equations [24]:

$$\log W = \log A - \frac{E_a}{2{,}303RT} \qquad (19)$$

$$\log\left(\frac{W}{T}\right) = \left[\log\left(\frac{R}{Nh}\right) + \frac{\Delta S^*_a}{2{,}303R}\right] - \frac{\Delta H^*_a}{2{,}303RT} \qquad (20)$$

W is the corrosion rate, R is the perfect gas constant, A is the pre-exponential factor, h is Planck's constant and N is Avogadro's constant, E_a activation energy, ΔH^*_a change in activation enthalpy and ΔS^*_a change in activation entropy. Fig. 5 shows the Arrhenius curves log W versus 1/T for copper in 1M HNO3 nitric acid solution without and with different concentrations of Atenolol. Straight lines are obtained with correlation coefficients (R^2 > 0.9). The slopes ($-\frac{E_a}{2{,}303R}$) of these straight lines are used to calculate the apparent activation energy (E_a). The values of the thermodynamic activation quantities are given in Table 3.

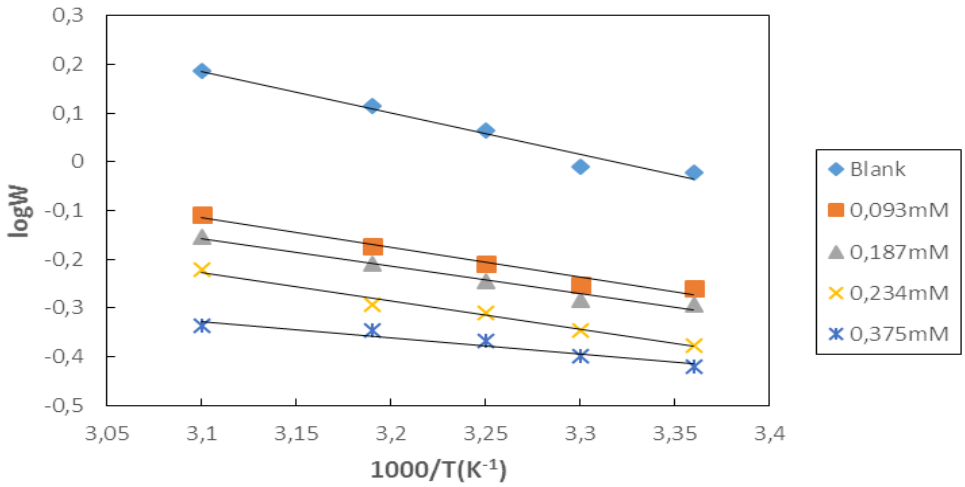

Fig. 5. log W versus 1/T for the corrosion of copper in 1M HNO_3 with and without atenolol

Table 3. Thermodynamic values of copper dissolution in 1M HNO_3 without and with different concentrations of Atenolol

Concentration (mM)	$E_a(kJ.mol^{-1})$	$\Delta H_a^*(kJ.mol^{-1})$	$\Delta S_a^*(J.mol^{-1}.K^{-1})$
0	16.39	13.80	-199.24
0,093	11.71	9.14	-219.46
0,187	10.68	8.17	-223.30
0,234	11.13	8.59	-223.33
0,375	6.39	3.83	-240

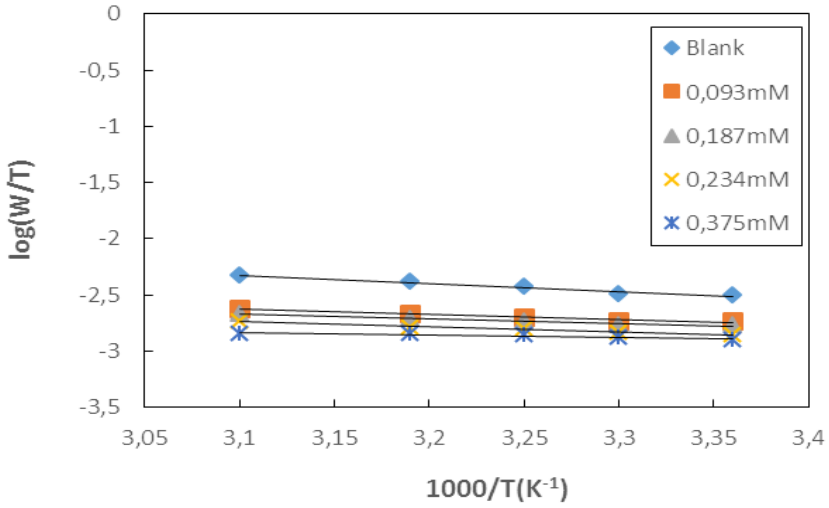

Fig. 6. log (W/T) versus 1/T for copper corrosion in 1M HNO_3 with and without Atenolol

The activation energy in the absence of Atenolol is higher than the activation energies in its presence; this would indicate according to the literature [25] that chemisorption is prevalent. Fig. 6 illustrates the log (W/T) versus 1/T.

The change in activation enthalpy ΔH_a^* is positive, indicating the endothermic nature of the copper dissolution. The activation entropy variation ΔS_a^* is negative, which would reflect [26] some organization during the formation of the activated complex.

3.4 Quantum Chemical Calculations Using the DFT Method

The calculations of the descriptors of the molecule were performed using density functional theory (DFT) at the B3LYP level with the 6-311 G (d,p) orbital basis. In this theory, based on the variational approach, the energy of the ground state is given by the relation:

$$E = \min_n[F(n) + \int d^3r\, V_{ext}(r)n(r)] \qquad (21)$$

After the structure optimization, the descriptor parameters of the molecule are calculated.

Fig. 7 shows the optimized molecular structure of atenolol.

Figs. 8 and 9 below give us the HOMO and LUMO densities of our molecule (atenolol) respectively.

The calculated quantum descriptors are reported in Table 4.

According to the literature [27], the energy E_{HOMO} (energy of the highest occupied orbital) is a reactivity parameter of molecules associated with the ability to donate electrons. A high value of E_{HOMO} would favour the tendency for a molecule to donate electrons to a suitable acceptor with a low energy vacant orbital. The observed E_{HOMO} value, (-5.902eV) for atenolol attests to its ability to donate electrons to copper. The ability of a molecule to form bonds with a metal surface would also depend on the value of E_{LUMO} (energy of the lowest unoccupied orbital). The energy E_{LUMO} indicates the ability of the molecule to accept electrons [28]. In this case, the value (-0.302eV) for atenolol shows its tendency to also accept electrons . So, the binding ability of the inhibitor to the metal surface increases with increasing E_{LUMO} and decreasing E_{HOMO}.

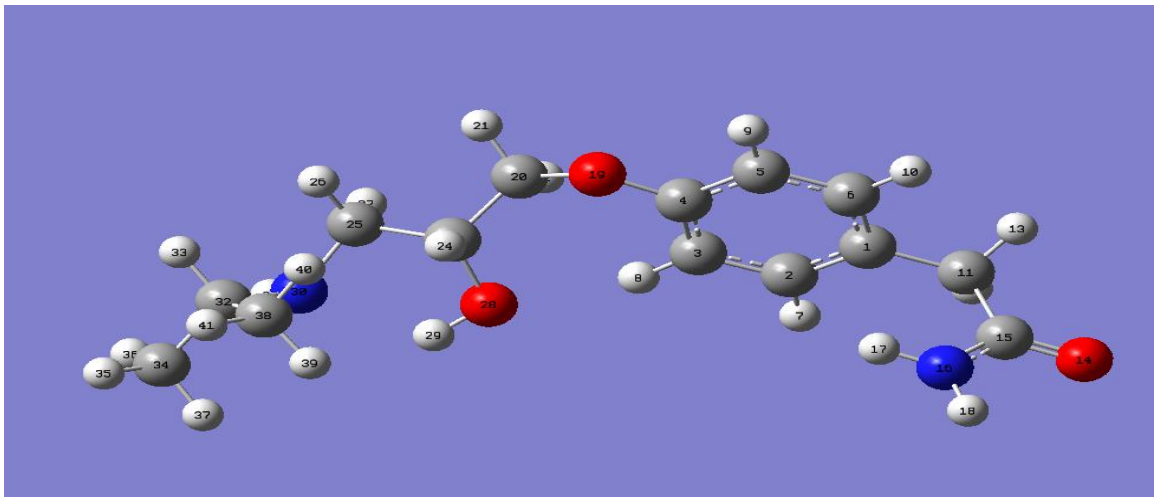

Fig. 7. Molecular structure of atenolol obtained from B3LYP/6-311G (d, p)

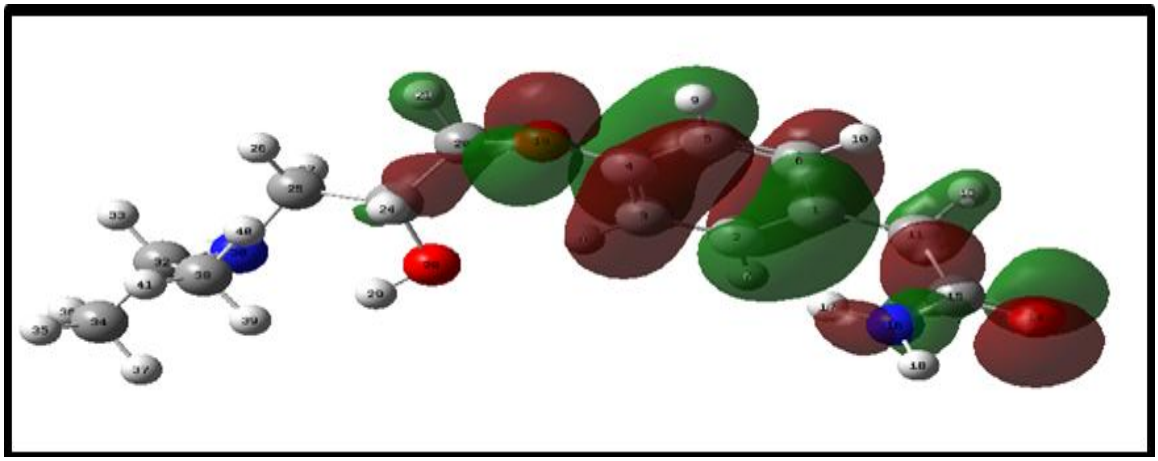

Fig. 8. HOMO density of atenolol at B3LYP/6-311G(d,p)

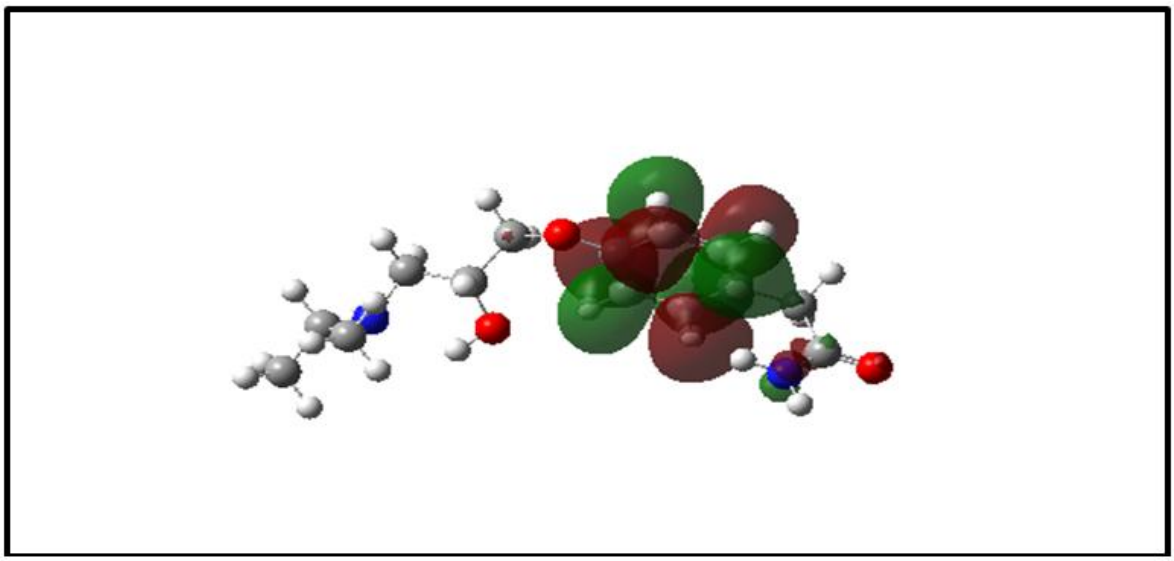

Fig. 9. LUMO density of atenolol at B3LYP/6-311G(d,p)

Table 4. Atenolol descriptor parameters obtained from B3LYP/6-311G (d,p)

Paramètres	Valeurs	Paramètres	Valeurs
E_{HOMO} (eV)	-5,902	χ (eV)	3,102
E_{LUMO} (eV)	-0,302	η (eV)	2,800
ΔE (eV)	5,600	S (eV)$^{-1}$	0,357
μ (Debye)	8,527	ΔN	0,335
I (eV)	5,902	ω (eV)	1,718
A (eV)	0,302	μ (eV)	-3,102

The energy gap value $\Delta E = E_{LUMO} - E_{HOMO}$ is also an important reactivity parameter for organic molecules. Low values of ΔE would favour exchanges between the molecules and the metal. It has been proved that molecules with ΔE value of the order of 5eV are good inhibitors [29]. In our case, the low value of ΔE (5.600eV) for atenolol confirms the experimental results obtained. This value of ΔE allows us to affirm that between our atenolol molecule and the metal copper, the electron displacement is more easily done from the molecule towards the metal.

The overall softness (s) and the overall hardness (η) are also important reactivity parameters that provide information on the likely ability of a molecule to interact with a metal surface [30].

They measure molecular stability as well as molecular reactivity. A hard molecule has a large energy gap and a soft molecule has a small energy gap. A good inhibitor has a high softness value and a low hardness value (low ΔE). The results show that atenolol has low hardness values (η=2.800 eV) and therefore a high softness [s = 0.357(eV)$^{-1}$] compared to those found in the literature [31]. This value reflects the experimental results.

The ionization energy is also an important descriptor of the chemical reactivity of atoms and molecules. A high ionization energy indicates high stability while a low value is associated with high reactivity of atoms and molecules [32].

In our case, the low ionization energy (5.902 eV) surely explains the good inhibitory power of atenolol compared to those found in the literature [31].

Generally, the number of transferred electrons (ΔN) can be used to show the electron donating capacity of the inhibitor [33]. According to the literature a value of ΔN<3.6 eV means that corrosion inhibition occurs in increasing order of (ΔN) values [33].

This is the case in our study as we obtained ΔN = 0.335 eV. This comparison can be made here because our descriptors correspond to the ground state and the experimental values are determined for temperatures starting at 298K.

The electrophilicity index (ω) which is another important parameter for understanding the behaviour of molecules, expresses the ability of the inhibitor to receive electrons from the metal. In our study, the value of the electrophilicity index (ω =1.718 eV) indicates that atenolol has the ability to accept electrons from copper [31]. These results explain the nature of the type of adsorption (chemisorption) obtained.

The dipole moment (μ) is related to the distribution of electronic charges in the molecule. It is also an important parameter that reflects the ability of the molecule to adsorb to the surface of a metal. In our case, the value of this parameter is high (μ=8.527 Debye). According to some authors [31,34], the ability of a molecule to adsorb to the surface of a metal is all the greater as its dipole moment is high.

The values of the Fukui function and the local softness of the electrophilic and nucleophilic attack sites are gathered in Table 5.

The analysis of the values of the functions recorded in the above table for the inhibitor, allows us to deduce that the nucleophilic attacks take place around the carbon atom C(3) (nucleophilic attack centre, included in the LUMO density zone) as possessing the largest values of f_k^+ and also possessing the largest value of $\boldsymbol{\Delta f}(\vec{r}) > 0$. The electrophilic attacks occur around the oxygen atom O(19) (electrophilic attack centre, included in the HOMO density region) as it possesses the largest values of $f_k^-(r)$ and of $\boldsymbol{\Delta f}(\vec{r}) > 0$ in absolute value.

Table 5. Fukui function values and local softnesses for Atenolol

Atome	f_k^+	f_k^-	s_k^+	s_k^-
C1	0,043	0,075	0,015	0,027
C2	0,096	0,039	0,034	0,014
C3	**0,149**	0,006	**0,053**	0,002
C4	-0,026	0,087	-0,009	0,031
C5	0,107	0,066	0,038	0,024
C6	0,090	0,025	0,032	0,009
C11	0,025	-0,044	0,009	-0,016
O14	0,078	0,114	0,028	0,041
C15	-0,060	0,063	-0,021	0,022
N16	0,042	-0,007	0,015	0,002
O19	-0,011	**0,137**	-0,004	**0,049**
C20	0,003	-0,017	0,001	0,006
C23	0,020	-0,023	0,007	-0,008
C25	0,013	-0,009	0,005	-0,003
O28	0,019	-0,025	0,007	-0,009
N30	0,034	0,032	0,012	0,011
C32	0,008	-0,020	0,003	0,007
C34	0,018	-0,012	0,006	-0,004
C38	0,003	-0,002	0,001	-0,001

4. PROPOSED MECHANISM SHOWING THE PREPONDERANCE OF CHEMISORPTION

The experimental (inhibitory efficiency) and theoretical results (the fraction of transferred electrons ΔN, the Fukui index f_k^α and the dual descriptors Δf) obtained in our studies suggest a physical barrier consisting of a complex obtained by electron transfers from the most probable centre for electrophilic attacks (centre for which the value of f_k^- is maximum and the value of $\Delta f(\vec{r}) < 0$¶ in absolute value is maximum and belonging to the HOMO zone) towards the incomplete orbitals of Cu^{2+} ions:

$$\text{Inh} \dashrightarrow \text{Cu}^{2+}\ [\text{Cu} - \text{Inh}] \quad (12)$$

The molecules could receive electrons from the copper (d) orbitals at the most likely centre for nucleophilic attack (centre for which the value of f_k^+ is maximum belonging to the LUMO zone) which would strengthen the link between the metal and the molecule

$$\text{Inh} \dashleftarrow \text{Cu}^{2+}\ [\text{Cu} - \text{Inh}]$$

These electron transfers justify the existence of the chemisorption phenomenon which is preponderant in the adsorption process of molecules on the copper surface.

The figure below is a proposed diagram of the inhibition mechanism:

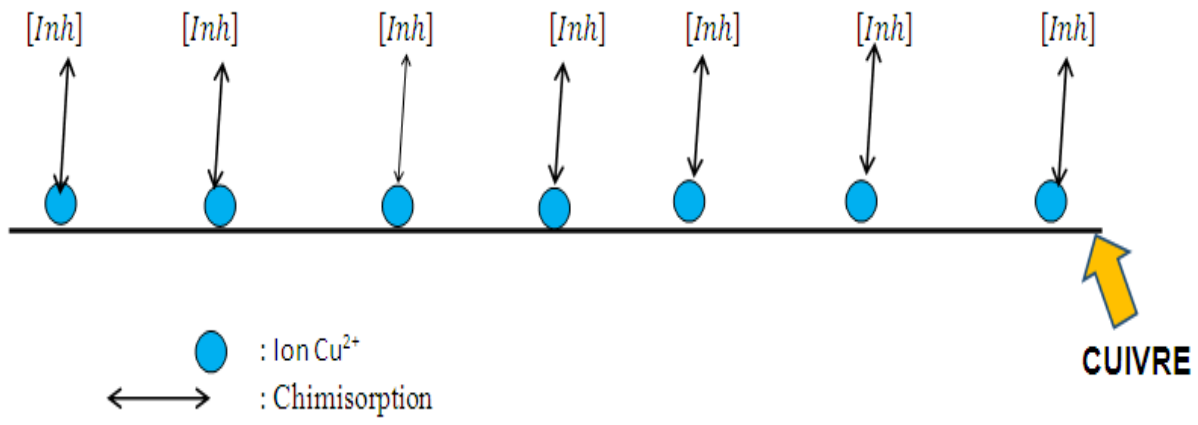

5. CONCLUSION

This study showed that the inhibitory efficacy of atenolol increases with both concentration and temperature. Atenolol adsorbs to copper according to the modified Langmuir isotherm. Also, the calculated thermodynamic parameters related to adsorption and activation show the existence of two types of adsorption but chemisorption is preponderant. The quantum chemical parameters confirm the inhibition efficiency of Atenolol. Atenolol acts as a good inhibitor of copper corrosion in 1M nitric acid.

ACKNOWLEDGEMENTS

Our thanks to the different Directors of the Laboratories of Thermodynamics and Physico-Chemistry of the environment of the University NANGUI ABROGOUA, Professor ZIAO NAHOSSE and of Constitution and Reaction of the matter of the University Félix Houphouët Boigny (Ivory Coast), Professor TROKOUREY ALBERT.

COMPETING INTERESTS

Authors have declared that no competing interests exist.

REFERENCES

1. Fouda AS, Eldesoky AM, Diab MA, et al. Inhibitive, adsorption studies on carbon steel corrosion in acidic solutions by new synthesized benzene sulfonamide derivatives. Int. J. Electrochem. Sci. 2016; 11:9998-10019.
2. Sherif ESM. Effects of 2-amino-5-(ethylthio)-1, 3, 4-thiadiazole on copper corrosion as a corrosion inhibitor in 3% NaCl solutions. Applied Surface Science. 2006;252(24):8615-8623.
3. Nunez L, Reguera E, Corvo F, Gonzalez E, Vazquez C. Corrosion of copper in seawater and its aerosols in a tropical island. Corrosion Science. 2005;47(2): 461-484.
4. Christy AG, Lowe A, Otieno-Alego V, Stoll M, Webster RD. Voltammetric and Raman microspectroscopic studies on artificial copper pits grown in simulated potable water. Journal of Applied Electrochemistry. 2004;34(2):225-233.
5. Zhang DQ, Gao LX, Zhou GD. Inhibition of copper corrosion by bis-(1-benzotriazolymethylene)-(2, 5-thiadiazoly)-disulfide in chloride media. Applied Surface Science. 2004;225(1-4):287-293.
6. Otmačić H, Telegdi J, Papp K, Stupnišek-Lisac E. Protective properties of an inhibitor layer formed on copper in neutral chloride solution. Journal of Applied Electrochemistry. 2004;34(5):545-550.
7. Otmačić H, Stupnišek-Lisac E. Copper corrosion inhibitors in near neutral media. Electrochimica Acta. 2003;48(8):985-991.
8. Scendo M, Poddebniak D, Malyszko J. Indole and 5-chloroindole as inhibitors of anodic dissolution and cathodic deposition of copper in acidic chloride solutions. Journal of Applied Electrochemistry. 2003; 33(3):287-293.
9. Fontana MG, Staehle KW. Advances in corrosion Science et Technology, vol 1, Plenum Press, New York; 1970.
10. Al-Otaibi MS, Al-Mayouf AM, Khan M, Mousa AA, Al-Mazroa SA, Alkhathlan HZ. Corrosion inhibitory action of some plant extracts on the corrosion of mild steel in acidic media. Arabian Journal of Chemistry. 2014;7(3):340-346.
11. Morad MS. Inhibition of iron corrosion in acid solutions by Cefatrexyl: Behaviour near and at the corrosion potential. Corrosion Science. 2008;50(2):436-44.
12. Geerlings P, De Proft F, Langenaeker W. Conceptual density functional theory. Chemical Reviews. 2003;103(5):1793-1874.
13. Dennington R, Keith T, Millam J. Gauss view version 5, Semichem Inc., Shawnee Mission, KS; 2009.
14. Frisch MJEA, Trucks GW, Schlegel HB, Scuseria GE, Robb MA, Cheeseman JR, Fox DJ. Gaussian 09, Revision d. 01, Gaussian. Inc., Wallingford CT. 2009;201.
15. Parr RG, Donnelly RA, Levy M, Palke WE. Electronegativity: the density functional viewpoint. The Journal of Chemical Physics. 1978;68(8):3801-3807.
16. Koopmans T. Über die Zuordnung von wellenfunktionen und eigenwerten zu den einzelnen elektronen eines atoms. Physica. 1934;1(1-6):104-113.
17. Pearson RG. Hard and soft acids and bases. Journal of the American Chemical Society. 1963;85(22):3533-3539.
18. Yang W, Parr RG. Hardness, softness, and the fukui function in the electronic theory of metals and catalysis. Proceedings of the National Academy of Sciences. 1985; 82(20):6723-6726.

19. Parr RG, Szentpály LV, Liu S. Electrophilicity index. Journal of the American Chemical Society. 1999;121(9): 1922-1924.
20. Yin S, Woo HC, Choi JH, Park YB, Chun BS. Measurement of antioxidant activities and phenolic and flavonoid contents of the brown seaweed Sargassum horneri: comparison of supercritical CO_2 and various solvent extractions. Fisheries and Aquatic Sciences. 2015;18(2):123-130.
21. Villamil RF, Corio P, Agostinho SM, Rubim JC. Effect of sodium dodecylsulfate on copper corrosion in sulfuric acid media in the absence and presence of benzotriazole. Journal of Electroanalytical Chemistry. 1999;472(2):112-119.
22. Moretti G, Guidi F, Grion G. Tryptamine as a green iron corrosion inhibitor in 0.5 M deaerated sulphuric acid. Corrosion Science. 2004;46(2):387-403.
23. Ahamad I, Quraishi MA. Bis (benzimidazol-2-yl) disulphide: an efficient water soluble inhibitor for corrosion of mild steel in acid media. Corrosion Science. 2009;51(9): 2006-2013.
24. Niamien PM. Copper Corrosion Inhibition in 1 M Nitric Acid: Adsorption and Inhibitive Action of Theophylline.
25. Nwabanne JT, Okafor VN. Inhibition of the corrosion of mild steel in acidic medium by Vernonia amygdalina: adsorption and thermodynamics study. Journal of Emerging trends in Engineering and Applied Sciences. 2011;2(4):619-625.
26. Zarrouk A, Hammouti B, Al-Deyab SS, Salghi R, Zarrok H, Jama C, Bentiss F. Corrosion inhibition performance of 3, 5-diamino-1, 2, 4-triazole for protection of copper in nitric acid solution. Int. J. Electrochem. Sci. 2012;7(7):5997-6011.
27. Dewar MJS, Thiel W. Ground states of molecules, 38. The MNDO Method. Approximations and Parameters. J. Am. Chem. Soc. 1977;99:4899.
28. Gece G, Bilgic S. Quantum chemical study of some cyclic nitrogen compounds as corrosion inhibitor of steel in NaCl media, Corros. Sci. 2009;51: 1876.
29. Niamien PM, Essy FK, Trokourey A, Yapi A, Aka HK, Diabaté D. Correlation between the molecular structure and the inhibiting effect of some Benzimidazole derivatives, Materials Chemistry and Physics. 2012;136:59-65.
30. Obi-Egbedi NO, Obot IB, El-Khaiary MI, Umoren SA, Ebenso EE. Computational simulation and statistical analysis on the relationship between corrosion inhibition efficiency and molecular structure of some phenanthroline derivatives on mild steel surface. Int. J. Electrochem. Sci. 2011; 6(1):5649-5675.
31. Michaelson HB. The work function of the elements and its periodicity. J. Appl. Phys. 1977;48:4729.
32. Gece G. The use of quantum chemical methods in corrosion inhibitor studies, Corros. Sci. 2008;50:2981.
33. Lukovits I, Kalman E, Zucchi F. Corrosion inhibitors- Correlation between electronic structure and efficiency. Corrosion. 2001;57:3.
34. Ebenso EE, Isabirye DA, Eddy NO. Adsorption and quantum chemical studies on the inhibition potentials of some thiosemicarbazides for the corrosion of mild steel in acidic medium. Int. J. Mol. Sci. 2010;1:2473.

Peer-review history:
The peer review history for this paper can be accessed here:
https://www.sdiarticle4.com/review-history/74673